Sequential Assembly of Homogeneous Magnetic Prussian Blue Films on Templated Surfaces

Jeffrey T. Culp,[†] Ju-Hyun Park,[‡] Isa O. Benitez,[†] Young-Duk Huh,[†,§] Mark W. Meisel,[‡] and Daniel R. Talham*,[†]

Department of Chemistry, University of Florida, Gainesville, Florida 32611-7200, Department of Physics and Center for Condensed Matter Sciences, University of Florida, Gainesville, Florida 32611-8440, and from the Department of Chemistry, Dankook University, Seoul, 140-714, Korea

Received March 4, 2003. Revised Manuscript Received June 12, 2003

Thin homogeneous films of the Prussian blue analogues with idealized formulas $KFe^{III}[Fe^{II}(CN)_6]$, $KNi^{II}[Fe^{III}(CN)_6]$, $CsNi^{II}[Cr^{III}(CN)_6]$, and $KCr^{II}[Cr^{III}(CN)_6]$ have been prepared through the sequential adsorption of the appropriate metal ions and hexacyanometalate complexes onto hydrophobic surfaces that were first templated with an Fe−CN−Ni two-dimensional grid network deposited as a Langmuir−Blodgett monolayer. The template is essentially one layer of the cubic Prussian blue structure and provides a well-matched surface for the deposition of the bulk cubic solids. The effectiveness of the method is verified by the exceptional surface coverage indicated by atomic force microscopy (AFM) and scanning electron microscopy (SEM) studies. Grazing incidence X-ray diffraction (GIXD) using synchrotron radiation confirms the face-centered cubic structures of the product films. Magnetic measurements of the thin films prepared on Mylar substrates yield behavior similar to that observed in the analogous powders, with the $KFe^{III}[Fe^{II}(CN)_6]$, $KNi^{II}[Fe^{III}(CN)_6]$, and $CsNi^{II}[Cr^{III}(CN)_6]$ films ordering ferromagnetically with $T_c = 5$, 20, and 75 K, respectively. The $KCr^{II}[Cr^{III}(CN)_6]$ film orders ferrimagnetically at $T_c = 210$ K.

Introduction

Prussian blue (PB) is a cubic mixed-valent iron−cyanide polymer of approximate composition $Fe^{III}_4[Fe^{II}(CN)_6]_3 \cdot 14H_2O$.[1] An intense metal-to-metal charge-transfer absorbance band gives it a deep blue color, the intensity of which changes with oxidation state, leading to many investigations of Prussian blue as an electrochromic material.[2−5] Prussian blue (PB) and related compounds have also been investigated as potential cation sensors,[7−10] where defects in the cubic structure lead to a charge imbalance that is compensated by incorporating alkali cations.[6]

Recently, magnetic studies of PB derivatives have generated a great deal of interest.[6,11−22] The cubic PB structure is not limited to iron ions, and compositions can be varied to include combinations of several transition metal ions in different oxidation states. This synthetic versatility, coupled with the ability of the bridging cyanide ligand to efficiently mediate magnetic exchange, has led to several mixed-spin molecule-based magnetic systems,[12−14] including some which order well above room temperature.[15−18] Further interest

[†] Department of Chemistry, University of Florida.
[‡] Department of Physics and Center for Condensed Matter Sciences, University of Florida.
[§] Dankook University.

(1) Ludi, A.; Güdel, H. U. *Struct. Bonding* **1973**, *14*, 1.
(2) Mortimer, R. J. *Chem. Soc. Rev.* **1997**, *26*, 147−156.
(3) Itaya, K.; Uchida, I.; Neff, V. D. *Accounts Chem. Res.* **1986**, *19*, 162−168.
(4) Carpenter, M. K.; Conell, R. S. *J. Electrochem. Soc.* **1990**, *137*, 2464−2467.
(5) Duek, E. A. R.; Depaoli, M. A.; Mastragostino, M. *Adv. Mater.* **1992**, *4*, 287−291.
(6) Verdaguer, M.; Bleuzen, A.; Marvaud, V.; Vaissermann, J.; Seuleiman, M.; Desplanches, C.; Scuiller, A.; Train, C.; Garde, R.; Gelly, G.; Lomenech, C.; Rosenman, I.; Veillet, P.; Cartier, C.; Villain, F. *Coord. Chem. Rev.* **1999**, *192*, 1023−1047.
(7) a. Pyrasch, M.; Tieke, B. *Langmuir* **2001**, *17*, 7706−7709. b. Pyrasch, M.; Toutianoush, A.; Jin, W.; Schnepf, J.; Tieke, B. *Chem. Mater.* **2003**, *15*, 245−254.
(8) Xu, J. J.; Fang, H. Q.; Chen, H. Y. *J. Electroanal. Chem.* **1997**, *426*, 139−143.
(9) Bharathi, S.; Yegnaraman, V.; Rao, G. P. *Langmuir* **1995**, *11*, 666−668.
(10) Itaya, K.; Ataka, T.; Toshima, S. *J. Am. Chem. Soc.* **1982**, *104*, 4767−4772.
(11) Dunbar, K. R.; Heintz, R. A. In *Progress in Inorganic Chemistry, Vol 45*; John Wiley and Sons: New York, 1997; Vol. 45, pp 283−391.
(12) Gadet, V.; Mallah, T.; Castro, I.; Verdaguer, M.; Veillet, P. *J. Am. Chem. Soc.* **1992**, *114*, 9213−9214.
(13) Mallah, T.; Thiebaut, S.; Verdaguer, M.; Veillet, P. *Science* **1993**, *262*, 1554−1557.
(14) Ferlay, S.; Mallah, T.; Ouahes, R.; Veillet, P.; Verdaguer, M. *Inorg. Chem.* **1999**, *38*, 229−234.
(15) Ferlay, S.; Mallah, T.; Ouahes, R.; Veillet, P.; Verdaguer, M. *Nature* **1995**, *378*, 701−703.
(16) Dujardin, E.; Ferlay, S.; Phan, X.; Desplanches, C.; Moulin, C. C. D.; Sainctavit, P.; Baudelet, F.; Dartyge, E.; Veillet, P.; Verdaguer, M. *J. Am. Chem. Soc.* **1998**, *120*, 11347−11352.
(17) Holmes, S. M.; Girolami, G. S. *J. Am. Chem. Soc.* **1999**, *121*, 5593−5594.
(18) Hatlevik, O.; Buschmann, W. E.; Zhang, J.; Manson, J. L.; Miller, J. S. *Adv. Mater.* **1999**, *11*, 914−918.
(19) Champion, G.; Escax, V.; Moulin, C. C. D.; Bleuzen, A.; Villain, F. O.; Baudelet, F.; Dartyge, E.; Verdaguer, N. *J. Am. Chem. Soc.* **2001**, *123*, 12544−12546.
(20) Escax, V.; Bleuzen, A.; Moulin, C. C. D.; Villain, F.; Goujon, A.; Varret, F.; Verdaguer, M. *J. Am. Chem. Soc.* **2001**, *123*, 12536−12543.
(21) Shimamoto, N.; Ohkoshi, S.; Sato, O.; Hashimoto, K. *Inorg. Chem.* **2002**, *41*, 678−684.
(22) Sato, O.; Iyoda, T.; Fujishima, A.; Hashimoto, K. *Science* **1996**, *272*, 704−705.

10.1021/cm034114w CCC: $25.00
Published on Web 08/01/2003

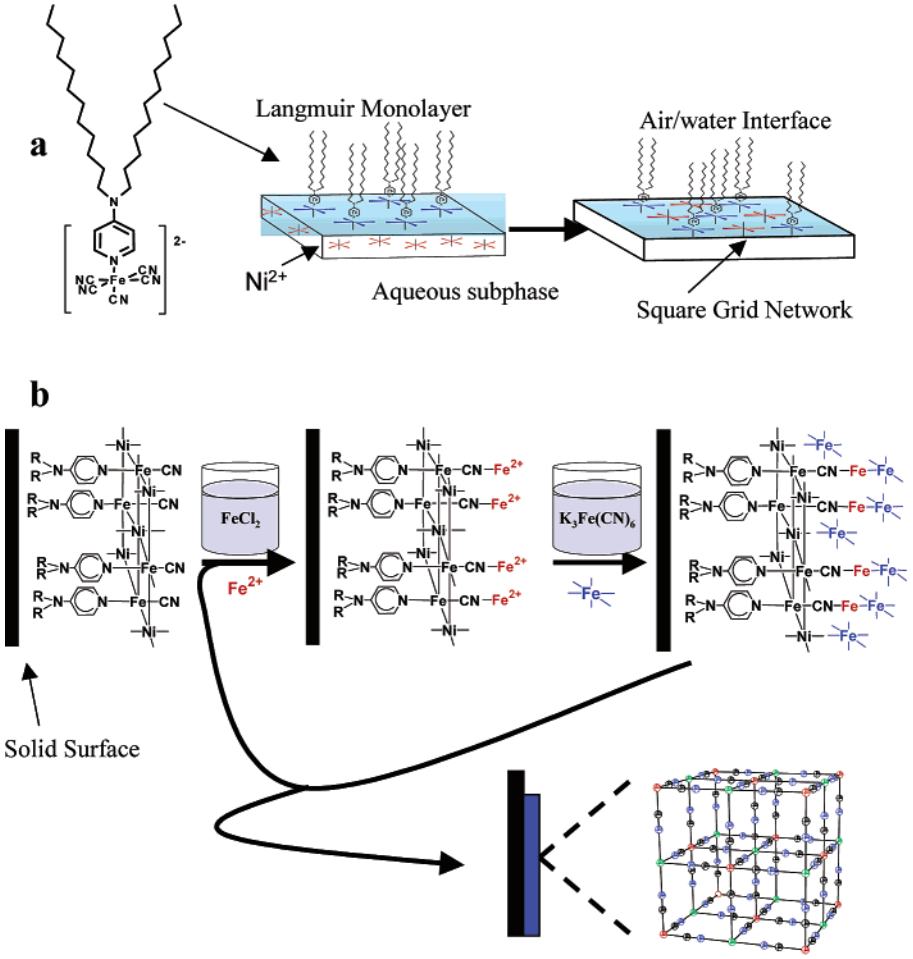

Figure 1. Scheme of the steps involved in the templated deposition of PB related films. (a) The template layer is preformed at the air/water interface. (b) After LB transfer of the template onto a hydrophobic support, the new surface is essentially one layer of the Prussian blue structure. Subsequent immersion in an aqueous solution of the appropriate metal ion followed by immersion in an aqueous solution of a hexacyanometalate complex results in the growth of a thin film of the polymeric metal cyanide. The cycle is repeated as necessary to achieve a homogeneous film.

has been generated by the observation of photoinduced magnetization changes in Fe−Co and Fe−Mn PB analogues.[19−22]

Many applications of PB related materials require homogeneous thin films, and several methods of depositing thin films onto solid supports have been reported. By far, the most commonly used technique is electrochemical deposition.[10,27−33] Other methods include adsorption onto sol−gel films,[23] adsorption at Langmuir monolayers,[24] and sequential deposition onto polyelectrolyte coated surfaces.[7,25,26] The morphologies of the deposited films vary, as the low solubility and poor crystallinity of most PB derivatives make surface wetting and the fabrication of continuous films difficult.

In this article, we report a new approach to thin homogeneous PB films that is modeled after the layer-by-layer deposition process commonly used for polyelectrolyte multilayers and is similar to the approach recently described by Millward et al.[26] and by Pyrasch and Tieke.[7a] An important variation described here is to first modify the surface with a monolayer of a two-dimensional iron−nickel−cyanide grid network. The two-dimensional grid network has been described previously,[34] and is essentially one layer of the cubic PB structure. By first providing a surface layer with chemistry and structure that is similar to PB, subsequent deposition of the bulk phase can wet the surface, resulting in continuous films at very thin coverage. The deposition process is depicted in Figure 1.

(23) Guo, Y. Z.; Guadalupe, A. R.; Resto, O.; Fonseca, L. F.; Weisz, S. Z. *Chem. Mater.* **1999**, *11*, 135−140.
(24) a. Lafuente, C.; Mingotaud, C.; Delhaes, P. *Chem. Phys. Lett.* **1999**, *302*, 523−527. b. Mingotaud, C.; Lafuente, C.; Amiell, J.; Delhaes, P. *Langmuir* **1999**, *15*, 289−292. c. Torres, G. R.; Agricole, B.; Delhaes, P.; Mingotaud, C. *Chem. Mater.* **2002**, *14*, 4012−4014. d. Torres, G. R.; Agricole, B.; Mingotaud, C.; Ravaine, S.; Delhaes, P. *Langmuir* **2003**, *19*, 4688−4693.
(25) Jaiswal, A.; Colins, J.; Agricole, B.; Delhaes, P., Ravaine, S. *J. Colloid Interface Sci.* **2003**, *261*, 330−335.
(26) Millward, R. C.; Madden, C. E.; Sutherland, I.; Mortimer, R. J.; Fletcher, S.; Marken, F. *J. Chem. Soc. Chem. Commun.* **2001**, 1994−1995.
(27) Buschmann, W. E.; Paulson, S. C.; Wynn, C. M.; Girtu, M. A.; Epstein, A. J.; White, H. S.; Miller, J. S. *Chem. Mater.* **1998**, *10*, 1386-1395.
(28) Neff, V. D. *J. Electrochem. Soc.* **1978**, *125*, 886−887.
(29) Lundgren, C. A.; Murray, R. W. *Inorg. Chem.* **1988**, *27*, 933−939.
(30) Kulesza, P. J.; Doblhofer, K. *J. Electroanal. Chem.* **1989**, *274*, 95−105.
(31) Kulesza, P. J.; Malik, M. A.; Miecznikowski, K.; Wolkiewicz, A.; Zamponi, S.; Berrettoni, M.; Marassi, R. *J. Electrochem. Soc.* **1996**, *143*, L10−L12.
(32) Sato, O.; Iyoda, T.; Fujishima, A.; Hashimoto, K. *Science* **1996**, *271*, 49−51.
(33) Gao, Z. Q. *J. Electroanal. Chem.* **1994**, *370*, 95−102.
(34) a. Culp, J. T.; Park, J. H.; Stratakis, D.; Meisel, M. W.; Talham, D. R. *J. Am. Chem. Soc.* **2002**, *124*, 10083−10090. b. Culp, J. T.; Park, J. H.; Meisel, M. W.; Talham, D. R. *Inorg. Chem.* **2003**, 2842−2848.

The template layer is prepared at the air−water interface of a Langmuir−Blodgett (LB) trough by spreading a monolayer of the amphiphilic pentacyanoferrate(III) complex, **1**, on a subphase containing divalent transition metal ions.[34] The resulting two-dimensional grid network has been well characterized.[34] The monolayer can then be transferred onto a hydrophobic support by using LB deposition techniques in such a way that the surface of the substrate becomes terminated with the reactive cyanides from the pentacyanoferrate complex, which are ideally organized in a two-dimensional face-centered grid motif. As such, the surface is well matched for subsequent epitaxial deposition of the bulk cubic solid via the sequential adsorption of aqueous metal ions, followed by cyanometalate ions. Characterization of the surface morphology using AFM and SEM indicates that the surface coverage is exceptional, and magnetic measurements reveal that the thin films possess bulk-like magnetic properties.

Experimental Section

Materials. Reagent grade $FeCl_2$, $Ni(NO_3)_2{\cdot}6H_2O$, $CrCl_2$, $K_3Fe(CN)_6$, $K_3Cr(CN)_6$, $Ag(NO_3)$, and CsI were purchased from Aldrich (Milwaukee, WI) and used without further purification. The salt $Cs_xK_{(3-x)}[Cr(CN)_6]$ was prepared by adding 25 mL of an aqueous solution containing 3.3 equiv (1.7 g, 10.0 mmol) of $Ag(NO_3)$ to 25 mL of an aqueous solution containing 1.0 g (3.1 mmol) of $K_3Cr(CN)_6$. The precipitated $Ag_xK_{(3-x)}Cr(CN)_6$ was collected by filtration, washed thoroughly with water, and suspended in a 20-mL aqueous solution of 3.2 g (12.4 mmol) of CsI. The solution was stirred vigorously at room temperature for 2 h and the AgI that formed was removed by filtration through Celite. Addition of 50 mL of absolute ethanol to the filtrate precipitated $Cs_xK_{(3-x)}[Cr(CN)_6]$ ($2.5 < x < 3.0$), which was collected by filtration and subsequently dried under vacuum in a desiccator (yield 1.4 g). The complex gave UV−Vis and IR spectra identical to those of the $K_3Cr(CN)_6$ starting material. The amphiphilic complex bis(tetramethylammonioum) pentacyano(4-didodecylaminopyridine)ferrate(III)$\cdot 6H_2O$ (**1**) was prepared as previously described.[34]

Instrumentation. UV−Vis spectra were obtained on a Hewlett-Packard 8452A diode array spectrophotometer. The LB films (template monolayers) were prepared with a KSV Instruments 5000 trough modified to operate with double barriers. The surface pressure was measured with a filter paper Wilhelmy plate suspended from a KSV microbalance. Subphase solutions were prepared from 17.8 to 18.1 MΩ cm water delivered with a Barnstead E-pure system. Magnetization measurements were performed on a Quantum Design MPMS SQUID magnetometer. Typical background scans from the Mylar supports and sample holder have been subtracted from the data.

Atomic force microscopy (AFM) imaging was performed using a Multimode AFM with a Nanoscope IIIa controller (Digital Instruments, Santa Barbara, CA) and commercially available silicon cantilever probes (Digital Instruments). Scanning electron microscopy (SEM) images were obtained with a Hitachi S-4000 FE-SEM at 6 kV.

Grazing incidence X-ray diffraction (GIXD) experiments using synchrotron radiation were performed at the Advanced Photon Source, Argonne, IL, at the Materials Research Collaborative Access Team beamline (sector 10).[35] The GIXD scans were performed on films prepared on glass slides. The samples were positioned in the center of an 8-circle Huber goniometer and oriented at an angle of 0.13° relative to the incident beam that was collimated to 200 μm high × 1500 μm wide and tuned to a wavelength of 1.254 Å. Diffracted intensity in the *xy* plane was measured using a NaI scintillation counter mounted on the Huber goniometer. The diffracted signal was collimated prior to the detector using Soller slits giving an experimental resolution on the order of 0.015 $Å^{-1}$.

Film Preparation. AFM, SEM, UV−Vis, and GIXD samples were prepared either on glass slides that were purchased from Buehler Ltd (Lake Bluff, IL) or on glass coverslips purchased from Fisher Scientific. Samples for SQUID investigations were prepared on Mylar substrates cleaned prior to use with absolute ethanol. The glass substrates were cleaned using the RCA procedure[36] and made hydrophobic by deposition of a monolayer of octadecyltrichlorosilane (OTS).[37,38]

Formation of the Template Layer. The amphiphilic iron complex **1** was spread from a chloroform solution onto the surface of a subphase 1 g/L in $Ni(NO_3)_2{\cdot}6H_2O$. All template monolayer films of the nickel−iron−cyanide network were transferred with one downstroke onto hydrophobic substrates at a surface pressure of 25 mN/m. The average transfer ratios were better than 0.9.

Deposition of the Prussian Blue Films. The bulk Prussian blue film is assembled onto the templated substrate by a sequential deposition process. After transfer of the template layer by the LB method, the substrate was removed from the trough and rinsed briefly with water. The substrate was then immersed in the appropriate 0.01 M aqueous $FeCl_2$, $Ni(NO_3)_2{\cdot}6H_2O$, or $CrCl_2$ solution for ∼1 min, then rinsed twice by brief immersion in two separate beakers of Nanopure water, then rinsed once by immersion in methanol, and finally dried under a stream of nitrogen before the process was repeated with an aqueous solution 0.01 M in the appropriate $K_3Fe(CN)_6$ or $K_3Cr(CN)_6$ complex salt. The $Cr^{II}/[Cr^{III}(CN)_6]$ film was prepared under a N_2 atmosphere with N_2-purged solutions. A $Cs_xK_{(3-x)}[Cr(CN)_6]$ solution 10 mM in $CsNO_3$ was used in the synthesis of the $Ni^{II}/[Cr^{III}(CN)_6]$ film. One deposition cycle consists of one immersion in each of the metal ion solutions.

Results and Discussion

Film Deposition. Figure 1 illustrates the deposition of a Prussian blue film, but the method is general, and combinations of different aqueous metal salts and cyanometalate complexes can be substituted for the ions shown in the scheme. Films based on Ni^{2+} and $[Cr(CN)_6]^{3-}$, Ni^{2+} and $[Fe(CN)_6]^{3-}$, and Cr^{2+} and $[Cr(CN)_6]^{3-}$ are also describe here. These solids generally contain alkali ions to balance the charge and metal ion vacancies that lead to incorporation of ligated water. A general formula for PB solids based on divalent metal ions, A^{2+}, and trivalent hexacyanometalate complexes, $[B(CN)_6]^{3-}$, is $C_jA_k[B(CN)_6]_l{\cdot}nH_2O$, where C is usually K^+ or Cs^+. The *k*/*l* ratio is not controlled in the deposition process described here, but is normally in the range $1 < {}^{k}/_{l} < {}^{3}/_{2}$. Throughout this paper the terminology $A^{II}/[B^{III}(CN)_6]$ will be used to refer to films of this composition generated from ions $A^{2+}{}_{(aq)}$ and complexes $[B(CN)_6]^{3-}{}_{(aq)}$. The exception is the film formed from $Fe^{2+}{}_{(aq)}$ and $[Fe(CN)_6]^{3-}$ which undergoes charge transfer to form a film based on $Fe^{III}/[Fe^{II}(CN)_6]$.

The deposition begins with the LB template layer that is formed by the reaction of a Langmuir monolayer of complex **1** with aqueous Ni^{2+} ions originating in the subphase. Nickel ions were used to form the template layer because the $Fe^{III}-CN-Ni^{II}$ grid formed this way has the highest structural coherence of the networks we have previously prepared with **1**, and its cell edge

(35) See http://ixs.csrri.iit.edu/mrcat/ for additional information.

(36) Kern, W. *J. Electrochem. Soc.* **1990**, *137*, 1887−1892.
(37) Maoz, R.; Sagiv, J. *J. Colloid Interface Sci.* **1984**, *100*, 465−496.
(38) Netzer, L.; Sagiv, J. *J. Am. Chem. Soc.* **1983**, *105*, 674−676.

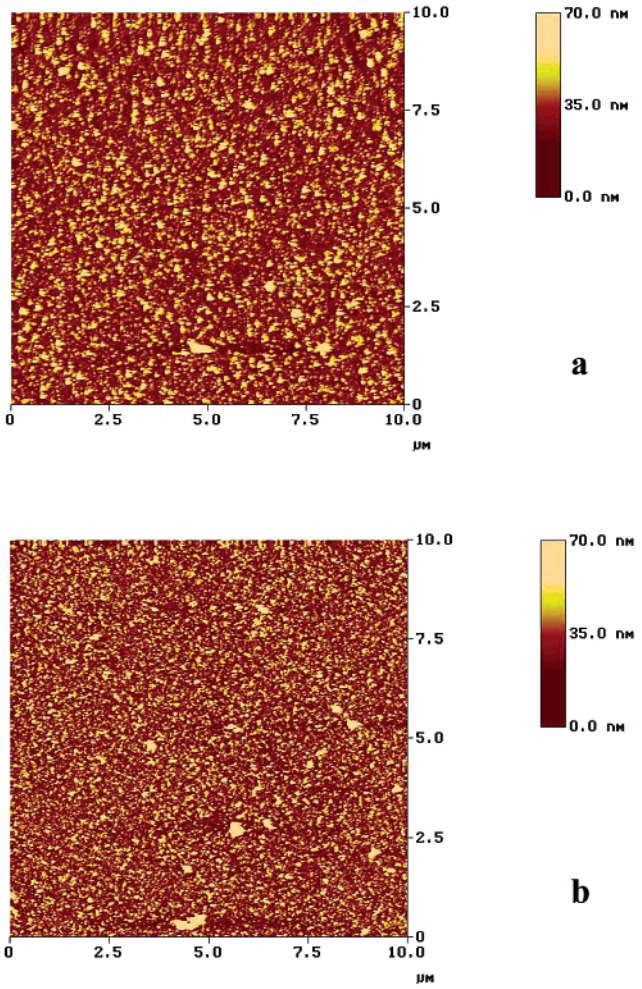

Figure 2. AFM images of (a) a $Ni^{II}/[Cr^{III}(CN)_6]$ film after 3 deposition cycles, and (b) an $Fe^{III}/[Fe^{II}(CN)_6]$ film after 5 deposition cycles. Both films were prepared on glass coverslips as described in the text.

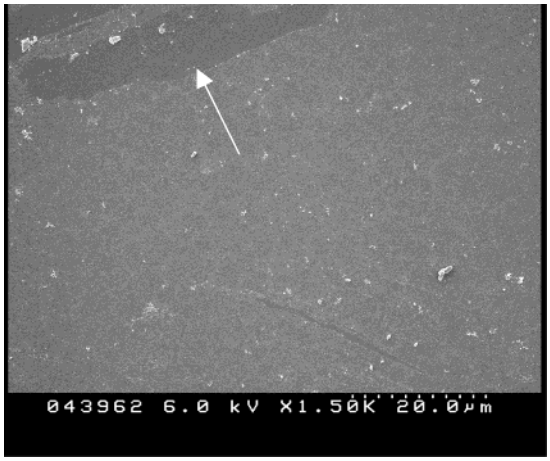

Figure 3. SEM image of an $Fe^{III}/[Fe^{II}(CN)_6]$ film after 10 cycles. The film was prepared on a glass coverslip as described in the text. An abrasion (indicated with the arrow) illustrates that the film is continuous elsewhere.

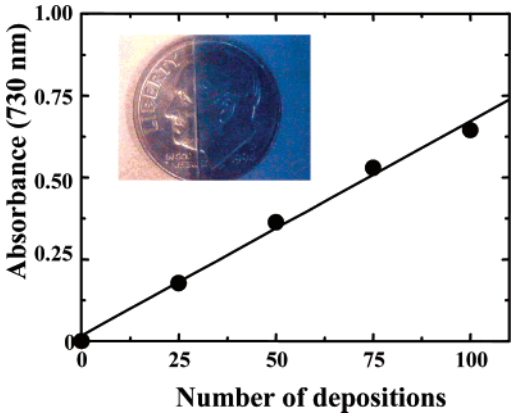

Figure 4. Linear fit to the absorbance at 730 nm versus deposition cycle for the $Fe^{III}/[Fe^{II}(CN)_6]$ film prepared on glass, through 100 cycles. Inset: A photograph demonstrating the transparency of an $Fe^{III}/[Fe^{II}(CN)_6]$ film after 100 deposition cycles.

of 10.2 Å is in the middle of the range normally expected for bulk PB derivatives.[34] The monolayer is then transferred to a hydrophobic surface, such as Mylar, or a piece of glass silanized with octadecyltrichlorosilane (OTS). The template is transferred so that the inorganic network is oriented away from the support, providing the surface with the character of the metal cyanide network. The substrates are then cycled through solutions of the appropriate metal ion and metal-complex building blocks to build up a thin film of the bulk solid.

Two AFM topography images, typical of the films prepared by Figure 1, are shown in Figure 2. Figure 2a is an image of a $Ni^{II}/[Cr^{III}(CN)_6]$ film after 3 deposition cycles, and Figure 2b is an image of an $Fe^{III}/[Fe^{II}(CN)_6]$ film after 5 deposition cycles. Both films were prepared on glass coverslips made hydrophobic with OTS. The images show complete surface coverage over the 100 μm^2 areas pictured. The lower (darker) background in both images was verified as the metal-cyanide film by comparing it to other images taken at defect sites (Supporting Information). The higher (lighter) regions in both films are due to particles on the surface and indicate that growth does not proceed by the idealized ionic-layer-by-ionic-layer process indicated in Figure 1. This conclusion is also supported by the ~30-nm average thickness of the 5-cycle film (in Figure 2b), which is higher than would be expected for a cubic lattice with a 1-nm unit cell length.

Despite the nonideal growth, the surface coverage is complete because the film wets the entire surface. Prussian-blue and related networks do not stick well to glass, and in the absence of any priming of the surface, precipitation occurs at isolated islands that coalesce as they grow to eventually complete coverage (Supporting Information). In contrast, the LB template layer facilitates uniform growth from the beginning of the deposition process.

Further evidence for complete surface coverage is provided by SEM, and an image of an $Fe^{III}/[Fe^{II}(CN)_6]$ film after 10 cycles is shown in Figure 3. Abrasions in the film clearly show the substrate below the film that is continuous over the remaining 400 μm^2. Similar results were obtained on the other metal−cyanide films. Although it does not grow one molecular layer at a time, the film deposits uniformly over large areas. Optical spectroscopy shows a linear increase in absorbance for the $Fe^{III}/[Fe^{II}(CN)_6]$ film through 100 deposition cycles, Figure 4. The 100-cycle film is colored but transparent (Figure 4 inset), further indicating the small grain size and the continuous coverage.

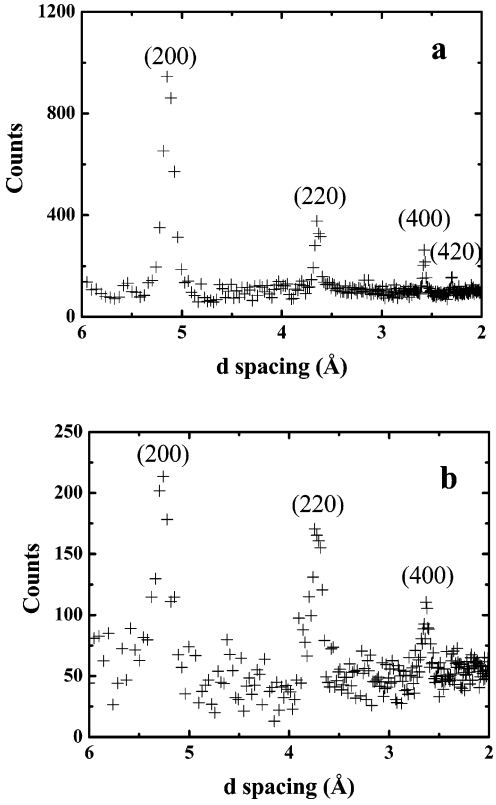

Figure 5. (a) GIXD pattern obtained for an $Fe^{III}/[Fe^{II}(CN)_6]$ film after 100 deposition cycles. The Miller indices are derived from a cubic unit cell with $a = 10.26$ Å. (b) GIXD pattern obtained for an $Ni^{II}/[Cr^{III}(CN)_6]$ film after 20 deposition cycles. The Miller indices are derived from a cubic unit cell with $a = 10.48$ Å.

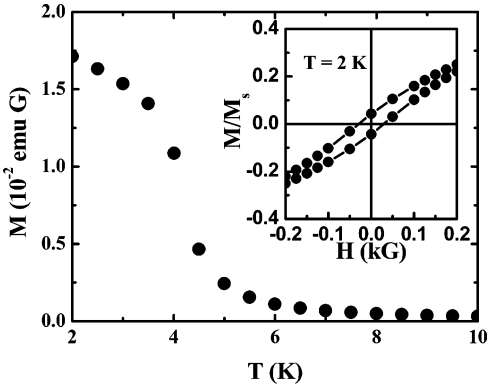

Figure 6. Field-cooled magnetization in 20 G as a function of temperature and hysteresis loop (inset) for a 10-cm^2 $Fe^{III}/[Fe^{II}(CN)_6]$ film after 100 deposition cycles.

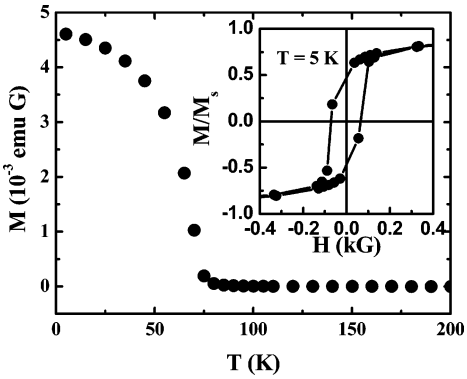

Figure 7. Field-cooled magnetization in 20 G as a function of temperature and hysteresis loop (inset) for an 8-cm^2 $Ni^{II}/[Cr^{III}(CN)_6]$ film after 20 deposition cycles.

The films were structurally characterized using grazing incidence X-ray diffraction from a synchrotron source.[34] The diffraction patterns obtained for an $Fe^{III}/[Fe^{II}(CN)_6]$ film after 100 deposition cycles and a $Ni^{II}/[Cr^{III}(CN)_6]$ film after 20 cycles are shown in Figure 5. Both diffraction patterns can be indexed to face-centered cubic cells with $a = 10.26$ Å for the $Fe^{III}/[Fe^{II}(CN)_6]$ structure and $a = 10.48$ Å for the $Ni^{II}/[Cr^{III}(CN)_6]$ structure. Both values are within the range typically observed for PB structures.[6,11,27,39] Analysis of the (200) peak widths for each pattern by application of the Scherrer equation[40] yields average structural coherence lengths of 190 Å and 150 Å for the $Fe^{III}/[Fe^{II}(CN)_6]$ and $Ni^{II}/[Cr^{III}(CN)_6]$ films, respectively.

Magnetism. Much of the current interest in PB family cyanometalates is due to their magnetic properties. Therefore, the magnetic response of each of the films prepared on Mylar substrates was measured as a function of temperature and applied field. Data for a 10 cm^2 film of $Fe^{III}/[Fe^{II}(CN)_6]$ after 100 deposition cycles are shown in Figure 6. The field-cooled magnetization vs temperature, $M_{fc}(T)$, shows a rapid rise at $T_c = 5$ K, and the film displays clear hysteresis at $T = 2$ K in the field-dependent magnetization, with a coercive field (H_c) of 30 G (Figure 6 inset). The behavior is consistent with ferromagnetic order in the film and is similar to bulk Prussian blue for which ferromagnetic order has been measured at $T_c = 5.6$ K by neutron scattering.[41]

Data for an 8 cm^2 film of $Ni^{II}/[Cr^{III}(CN)_6]$ after 20 deposition cycles are presented in Figure 7. The ferromagnetic ordering temperature, $T_c = 75$ K, is within the range of transition temperatures for previously reported $Ni^{II}/[Cr^{III}(CN)_6]$ salts. Ordering temperatures are sensitive to the ratio of Ni^{II} to Cr^{III}, with the highest value, $T_c = 90$ K, occurring for the 1:1 compound, $CsNi[Cr(CN)_6]\cdot 2H_2O$.[6,12] The lower ordering temperature of the film likely reflects a higher Ni:Cr ratio, as this is not controlled during the deposition process. An alternative reason for the lower ordering temperature might be reduced structural coherence, but the GIXD result shows reasonable coherence lengths for the film, suggesting the magnetic order is not suppressed by low crystallinity. Clear hysteresis is observed in the field dependent magnetization at 5 K, with $H_c = 70$ G and a remnant magnetization 50% of the saturation value. Both of these values are nearly identical to those reported by Gadet et al.[12] for $CsNi[Cr(CN)_6]\cdot 2H_2O$.

Figure 8 shows the magnetic data for a 6 cm^2 $Ni^{II}/[Fe^{III}(CN)_6]$ film after 10 deposition cycles. A transition to a ferromagnetic state is observed at $T_c = 18$ K. The ordering temperature is lower than the $T_c = 23.6$ K reported for the analogous solid,[42] and once again, most likely results from a slightly higher Ni:Fe ratio in the

(39) Buser, H. J.; Schwarzenbach, D.; Petter, W.; Ludi, A. *Inorg. Chem.* **1977**, *16*, 2704−2710.
(40) Guinier, A. *X-ray Diffraction*; Freeman: San Francisco, CA, 1968.
(41) Herren, F.; Fischer, P.; Ludi, A.; Halg, W. *Inorg. Chem.* **1980**, *19*, 956−959.
(42) Juszczyk, S.; Johansson, C.; Hanson, M.; Ratuszna, A.; Malecki, G. *J. Phys. Condes. Matter* **1994**, *6*, 5697−5706.

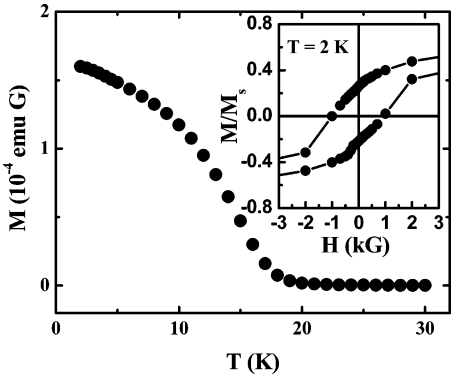

Figure 8. Field-cooled magnetization in 20 G as a function of temperature and hysteresis loop (inset) for a 6-cm^2 $Ni^{II}/[Fe^{III}(CN)_6]$ film after 10 deposition cycles.

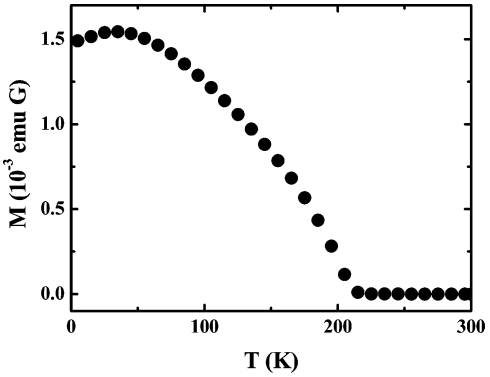

Figure 9. Field-cooled magnetization in 20 G as a function of temperature for a 7-cm^2 $Cr^{II}/[Cr^{III}(CN)_6]$ film after 40 deposition cycles.

film.[6] Magnetization vs field measured at $T = 2$ K reveals a coercive field, $H_c = 1000$ G.

To produce films with higher ordering temperatures, the deposition process was applied to $Cr^{II}/[Cr^{III}(CN)_6]$ as these PB analogues are known ferrimagnets with 150 K < T_c < 270 K, depending on the Cr^{II}:Cr^{III} ratio.[13,27,32] The $M_{fc}(T)$ for a 7 cm^2 $Cr^{II}/[Cr^{III}(CN)_6]$ film after 40 deposition cycles is shown in Figure 9. The data show the onset of long-range order at a $T_c = 215$ K, which is well within the reported range for $Cr^{II}/[Cr^{III}(CN)_6]$ compounds.[13,27,32]

Conclusions

A method for depositing Prussian blue family solids as thin, transparent, homogeneous films has been developed that uses a monolayer template to enhance surface wetting. The template is a two-dimensional cyanide-bridged grid network, preformed at the air−water interface before transfer to the solid support substrates. The technique yields films with virtually complete surface coverage as evidenced by AFM and SEM. The potential advantages of the method have been demonstrated with a series of mixed-metal cyanometalates to give transparent magnetic thin films with properties that are comparable to those of the powdered solid-state analogues.

Acknowledgment. This research was supported by the National Science Foundation through grant DMR-9900855 (D.R.T.) and by the American Chemical Society through grant ACS-PRF-36163-AC5 (M.W.M., D.R.T.). The NSF, through DMR-0113714, is further acknowledged for funding to acquire the SQUID magnetometer. Use of the Advanced Photon Source was supported by the U.S. Department of Energy, Office of Science, Office of Basic Energy Sciences, under Contract W-31-109-ENG-38. We also acknowledge support from the Materials Research Collaborative Access Team (MRCAT) at the Advanced Photon Source. The Electron Microscopy Core Laboratory, Biotechnology Program, University of Florida, is acknowledged for providing the instrumentation to record SEM images.

Supporting Information Available: AFM images and optical spectrum comparing Prussian blue deposited onto clean glass and glass primed with the LB template. This material is available free of charge via the Internet at http://acs.pubs.org.

CM034114W